

The crucial role of caspase-9 in the disease progression of a transgenic ALS mouse model

Haruhisa Inoue¹, Kayoko Tsukita¹,
Takuji Iwasato^{2,3}, Yasuyuki Suzuki¹,
Masanori Tomioka⁴, Minako Tateno¹,
Masahiro Nagao⁵, Akihiro Kawata⁵,
Takaomi C. Saido⁴, Masayuki Miura⁶,
Hidemi Misawa⁷, Shigeyoshi Itoharu²
and Ryosuke Takahashi^{1,8}

¹Laboratory for Motor System Neurodegeneration, ²Laboratory for Behavioral Genetics and ⁴Laboratory for Proteolytic Neuroscience, RIKEN Brain Science Institute (BSI), Saitama, ³PRESTO, Japan Science and Technology Corporation, Saitama, ⁵Department of Neurology, Tokyo Metropolitan Neurological Hospital, Tokyo, ⁶Department of Genetics, Graduate School of Pharmaceutical Sciences, University of Tokyo and ⁷Department of Neurology, Tokyo Metropolitan Institute for Neuroscience, Tokyo, Japan

⁸Corresponding author
e-mail: ryosuke@brain.riken.jp

Mutant copper/zinc superoxide dismutase (SOD1)-overexpressing transgenic mice, a mouse model for familial amyotrophic lateral sclerosis (ALS), provides an excellent resource for developing novel therapies for ALS. Several observations suggest that mitochondria-dependent apoptotic signaling, including caspase-9 activation, may play an important role in mutant SOD1-related neurodegeneration. To elucidate the role of caspase-9 in ALS, we examined the effects of an inhibitor of X chromosome-linked inhibitor of apoptosis (XIAP), a mammalian inhibitor of caspase-3, -7 and -9, and p35, a baculoviral broad caspase inhibitor that does not inhibit caspase-9. When expressed in spinal motor neurons of mutant SOD1 mice using transgenic techniques, XIAP attenuated disease progression without delaying onset. In contrast, p35 delayed onset without slowing disease progression. Moreover, caspase-9 was activated in spinal motor neurons of human ALS subjects. These data strongly suggest that caspase-9 plays a crucial role in disease progression of ALS and constitutes a promising therapeutic target.

Keywords: ALS/baculovirus p35/caspase/SOD1/XIAP

Introduction

Amyotrophic lateral sclerosis (ALS) is a neurodegenerative disorder resulting in progressive paralysis caused by motor neuron loss in the brain, brainstem and spinal cord. It is universally fatal, with a mean survival of 5 years after disease onset (for a review see Gurney *et al.*, 2000; Brown and Robberecht, 2001; Cleveland and Rothstein, 2001; Julien, 2001; Rowland and Shneider, 2001). Mutations in the human superoxide dismutase-1 (SOD1) are responsible

for an autosomal dominant form of familial ALS (Rosen *et al.*, 1993).

Accumulating evidence indicates that mutant SOD1 protein activity precipitates proapoptotic effects through its resulting abnormal function. Possible pathophysiological mechanisms in familial ALS associated with SOD1 mutation are the failure to fold or degrade mutant SOD1 (for a review see Gurney *et al.*, 2000; Brown and Robberecht, 2001; Cleveland and Rothstein, 2001; Julien, 2001; Rowland and Shneider, 2001), the formation of free radicals (for a review see Gurney *et al.*, 2000; Brown and Robberecht, 2001; Cleveland and Rothstein, 2001; Julien, 2001; Rowland and Shneider, 2001), the release of free copper (Hayward *et al.*, 2002; Subramaniam *et al.*, 2002), and/or a susceptibility to disulfide reduction of mutant SOD1 (Tiwari and Hayward, 2003). The resulting effects are subsequent axonal strangulation from neurofilamentous disorganization (for a review see Cleveland and Rothstein, 2001; Julien, 2001) and excitotoxic death due to mishandling of glutamate (Howland *et al.*, 2002). However, the precise mechanisms behind mutant SOD1-mediated neurotoxicity have yet to be unravelled.

The mutant SOD1 transgenic (mSOD1-Tg) mouse, a mouse model for familial ALS (Gurney *et al.*, 1994), provides the opportunity to elucidate the pathogenetic mechanisms underpinning ALS. The importance of apoptotic pathways in the pathogenesis of mSOD1-Tg mice is supported by the neuroprotective effects of several factors, including: Bcl-2 transgene (Kostic *et al.*, 1997), the dominant-negative caspase-1 transgene (Friedlander *et al.*, 1997), intraventricular administration of pan-caspase-inhibitor z-VAD-FMK (Li *et al.*, 2000) and feeding with minocycline (Zhu *et al.*, 2002). Caspase-1, -3, -7, -8 and -9 are also activated in the spinal motor neurons of mSOD1-Tg mice at various stages throughout the clinical course (Pasinelli *et al.*, 2000; Guégan *et al.*, 2001, 2002; for a review see Friedlander, 2003; Guégan and Przedborski, 2003). Moreover, cytochrome *c* release from mitochondria, which is also seen in mSOD1-Tg mice (Guégan *et al.*, 2001), activates caspase-9 in the presence of Apaf-1 which, in turn, activates downstream executioner caspases. These observations suggest that mitochondria-dependent apoptotic signaling, including caspase-9 activation, may play an important role in motor neuronal degeneration in mSOD1-Tg mice. However, the significance of caspase activation downstream of cytochrome *c* release has remained unclear.

To elucidate the role of caspase-9 in ALS, we used a transgenic approach to examine the effects of two different caspase inhibitory proteins, XIAP and p35, on the clinical course of mSOD1-Tg mice. XIAP, a mammalian protein, specifically inhibits caspase-3, -7 and -9; whereas p35, a baculoviral protein, inhibits a broad range of caspases, but not -9 (for a review see Deveraux and Reed, 1999; Ekert

et al., 1999; Yuan and Yankner, 2000; Suzuki *et al.*, 2001). When expressed using the same promoter, both proteins prolonged survival; however, human XIAP slowed disease progression without delaying its onset, while p35 delayed disease onset but did not affect its progression. These data strongly suggest that the inhibition of caspase-9 in motor neurons contributes significantly to attenuating the progression of ALS.

Results

Spinal motor neurons expressing either XIAP or p35

First we generated transgenic mice (XIAP-Tg) expressing human XIAP in spinal motor neurons, with glutamic acid substituted for aspartic acid in position 242 (D242E) under the control of the murine choline acetyltransferase (ChAT) promoter (Naciff *et al.*, 1999) (Figure 1A). Since ChAT is expressed only in matured neurons and a relatively specific marker protein for spinal motor neurons, we avoided developmental lethality caused by inhibiting apoptosis. The D242E mutant avoids cleavage by caspase-3 and is more resistant to Fas- or Bax-induced apoptosis than wild-type XIAP *in vitro* (Deveraux *et al.*, 1999). Human XIAP mRNA expression was detected in the spinal cords of XIAP-Tg lines (Figure 1B). Higher protein expressions were detected using western blot analysis in brain and spinal cord tissue in XIAP-Tg#4 mice compared with non-transgenic littermates (non-Tg) (Figure 1C). For our experiments we used the XIAP-Tg#4 line.

To express p35 in spinal motor neurons, transgenic (ChAT-Cre) mice expressing the P1-phage Cre recombinase were developed using a construct containing cDNA for Cre with a nuclear localization signal and the murine ChAT promoter (Figure 1D). Using CAG-CAT-Z reporter mice (Sakai and Miyazaki, 1997), we found that Cre/loxP recombination occurs in spinal motor neurons in ChAT-Cre#23 (data not shown). ChAT-Cre/loxP-p35 transgenic (p35-Tg) mice were generated by crossing ChAT-Cre#23 with loxP-p35 transgenic mice; in these mice, p35 gene expression is prevented because a stuffer sequence flanked by two loxP sequences is present (Figure 1D). p35 mRNA and protein expression were detected in p35-Tg mice spinal cords using RT-PCR (Figure 1E) and western blot analysis (Figure 1F). The p35 expressed by Cre/loxP recombination in our loxP-p35 transgenic mice reportedly inhibits caspases and associated cell death under various pathological conditions, including autoimmune-mediated demyelination *in vivo* (Hisahara *et al.*, 2000; Tomioka *et al.*, 2002; Viswanath *et al.*, 2002).

To confirm that XIAP in our XIAP-Tg mice functions as an inhibitor of cell death *in vivo* (Kügler *et al.*, 2000; Perrelet *et al.*, 2000; Crocker *et al.*, 2003), axotomy of the hypoglossal nerve was performed on adult female XIAP-Tg#4 mice. Axotomy-induced cell death was significantly suppressed, indicating that expressed XIAP was functional (Figure 1G). The effect of XIAP was similar to that of brain-derived neurotrophic factor (BDNF)-administration to the nerve stump ($p > 0.05$) (Figure 1G).

We used a line of mSOD1-Tg mice [G93A; glycine substituted for alanine at codon 93 of the human SOD1

protein (Gurney *et al.*, 1994)] as our ALS model. Female XIAP-Tg (or p35-Tg) mice were crossbred with male mSOD1-Tg mice to produce four varieties of mice: wild type (non-Tg), wild type (XIAP- or p35-Tg), mSOD1-Tg or mSOD1/(XIAP or p35)-Tg. Before investigating the neuroprotective effects of each transgene on mSOD1-Tg mice spinal cord, its expression in mutant SOD1 and human XIAP double transgenic (mSOD1/XIAP-Tg) [or mutant SOD1 and p35 double transgenic (mSOD1/p35-Tg)] mice was confirmed by immunohistochemistry (Figure 1H and I). As shown in Figure 1H (or I), the product of the transgene was expressed in spinal motor neurons of mSOD1/XIAP-Tg (or mSOD1/p35-Tg) mice.

XIAP and p35 prolong survival of the ALS mouse model differently

To determine the effects of XIAP or p35 transgenes on the onset and progression of motor neuron disease in mutant SOD1 mice, we compared the time of disease onset and life span between mSOD1-Tg and mSOD1/XIAP-Tg or mSOD1/p35-Tg mice. Onset was determined by the loss of motor function, which was measured using a rota-rod test. This occurred at a mean age of 242.0 ± 4.3 days in mSOD1/XIAP-Tg mice and at 236.3 ± 4.0 days in control mSOD1-Tg mice ($p > 0.05$) (Figure 2A). Onset of motor function loss was observed at a mean age of 257.1 ± 5.1 days in mSOD1/p35-Tg mice, compared with 235.1 ± 5.1 days in control mSOD1-Tg mice ($p = 0.0015$) (Figure 2B). Significantly, mean survival time was prolonged in both mSOD1/XIAP-Tg and mSOD1/p35-Tg mice. Mean survival for mSOD1/XIAP-Tg mice was 276.6 ± 4.8 days, whereas control mSOD1-Tg mice survived 258.9 ± 4.1 days ($p < 0.001$) (Figure 2A). Mean survival for mSOD1/p35-Tg mice was 281.9 ± 4.8 days, compared with 257.4 ± 4.6 days for control mSOD1-Tg mice ($p < 0.0005$) (Figure 2B).

Mean disease duration, the period marked by onset and death, was also assessed. Mean disease duration in mSOD1/XIAP-Tg mice was 34.6 ± 2.6 days, compared with 22.6 ± 1.7 days in control mSOD1-Tg mice ($p < 0.0005$). Mean disease duration in mSOD1/p35-Tg mice was 24.8 ± 2.3 days, compared with 22.3 ± 1.7 days in control mSOD1-Tg mice ($p > 0.05$). These data indicate that XIAP significantly extends survival of mSOD1-Tg mice by prolonging the duration of the disease, i.e. by ameliorating disease progression. In contrast, p35 extends survival by delaying disease onset.

We next assessed the effects of XIAP and p35 on spinal motor neuron death in mSOD1-Tg mice. At the end stage of mSOD1-Tg mice, ~30% of spinal motor neurons remained in mSOD1-Tg control mice compared with age-matched wild-type, XIAP-Tg and p35-Tg mice. In contrast, a significantly larger number of motor neurons were found in mSOD1/XIAP-Tg and mSOD1/p35-Tg than were found in mSOD1-Tg mice (Figure 3). As wild-type, XIAP-Tg and p35-Tg mice all have the same number of motor neurons, we can assume that that naturally occurring motoneuron death was not inhibited in these Tg mice.

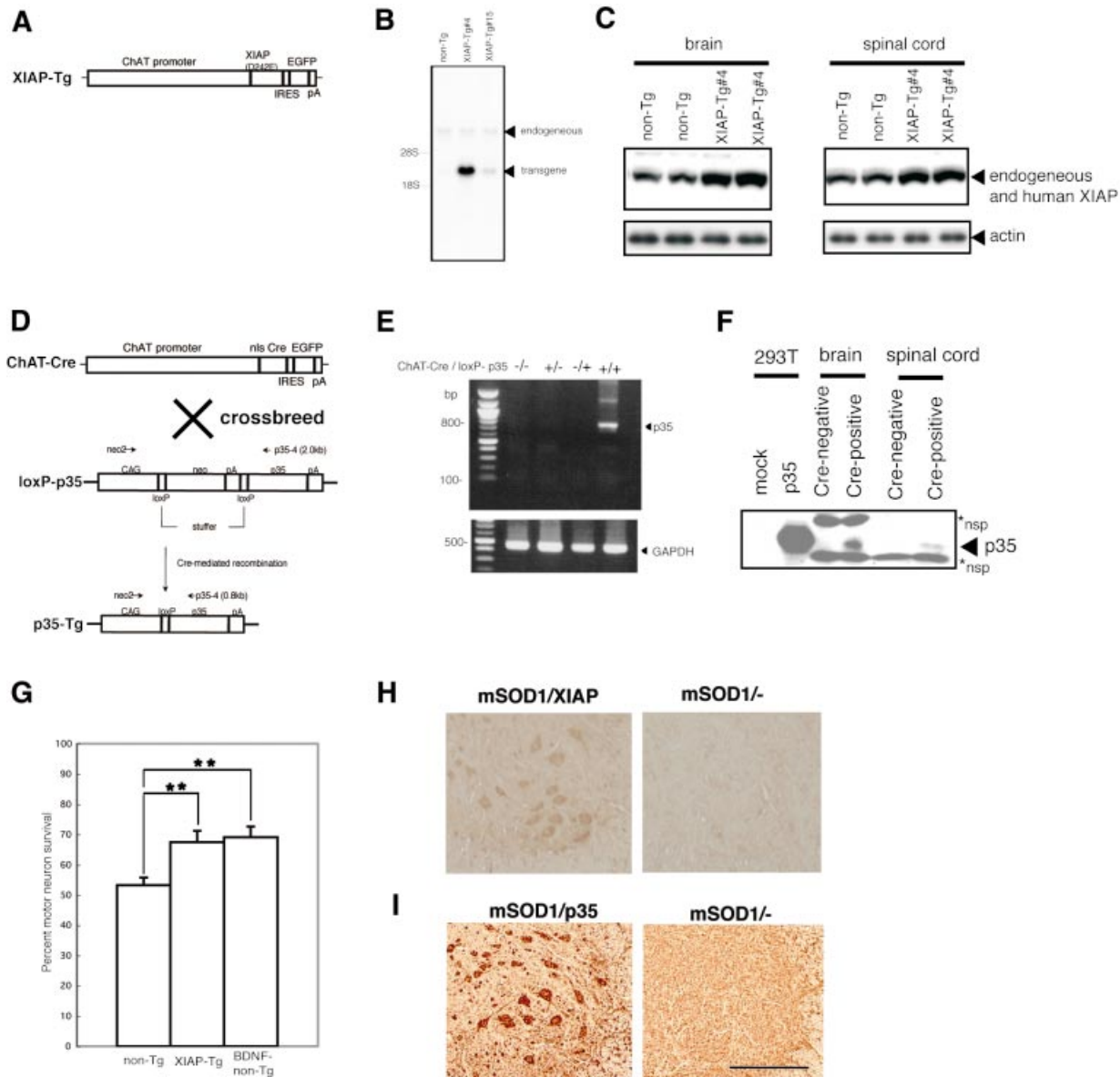


Fig. 1. (A) Diagram of the constructs of XIAP-Tg mice. (B) Representative autoradiograph of northern blot analysis showing transgenic human XIAP and endogenous XIAP mRNA levels in the spinal cord from one non-transgenic and two transgenic (XIAP-Tg#4 and -15) mouse lines. A cDNA of human XIAP from 913 to 1213 bp, with 86% identity with its mouse counterpart, was used as the probe. (C) Representative western blot analysis with anti-XIAP antibody that recognizes both human and mouse endogenous XIAP. Increased XIAP protein expression in XIAP-Tg brain and spinal cord tissue compared with non-transgenic littermates (non-Tg). (D and E) Schematic representation of the ChAT-Cre and loxP-p35 transgenes, and Cre-mediated removal of the neomycin stuffer. nls, nuclear localization signal; IRES, internal ribosome entry site; pA, polyadenylation signal. Cre recombinase excised the neomycin stuffer, allowing p35, which was positioned behind the second loxP sequence, to be expressed in ChAT-positive cells (e.g. spinal motor neurons). RT-PCR revealed p35 expression in spinal cord of a p35-Tg mouse. (F) Representative western blot analysis of p35 expression in brains and spinal cords of Cre-negative and -positive mice detected using anti-p35 antibody. p35 protein were expressed in both brain and spinal cord of p35-Tg. Extract of p35-overexpressing 293T cells was used as a positive control. *nsp, non-specific band. (G) Decreased axotomy-induced death of hypoglossal motor neurons in XIAP-Tg#4 mice. Percentage motor neuron survival is calculated as the ratio of the number of surviving motor neurons in axotomized hypoglossal nucleus to the number in the contralateral non-axotomized hypoglossal nucleus of XIAP-Tg, non-Tg littermates, and BDNF-administered non-Tg (BDNF-non-Tg) mice ($n = 6-7$ mice per group). An increase in the number of surviving motor neurons in XIAP-Tg, comparable to that of BDNF-non-Tg, is seen after axotomy compared with non-Tg mice (Tg, $67.5 \pm 3.7\%$; non-Tg, $53.2 \pm 2.5\%$; BDNF-non-Tg, $69.1 \pm 3.6\%$). ** $p < 0.01$ [calculated using to analysis of variance (ANOVA), followed by Fisher's test]. Error bars represent the standard error of the mean (SEM). (H and I) Expression of human XIAP or p35 in motor neurons of spinal cord is confirmed by immunohistochemistry using anti-human-specific XIAP antibody or anti-p35 antibody. mSOD1/XIAP-Tg mice showed strong immunoreactivity for human XIAP in spinal motor neurons. mSOD1/p35-Tg mice also expressed p35. Scale bar = 136 μ m.

Differential effects between XIAP and p35 depend on caspase-9

To explore the mechanisms underlying the effects of XIAP and p35, we examined caspase activation in spinal cords from mSOD1-Tg mice. Caspase-1 and -3 activation was

observed at an early stage in the clinical course of mSOD1-Tg mice (at 2 months), with a sharp drop in the level of procaspase-3 level at 6 months, 2 months before the onset (Figure 4A). Activated caspase-9 first appeared at 6 months, concomitant with a decrease of procaspase-9,

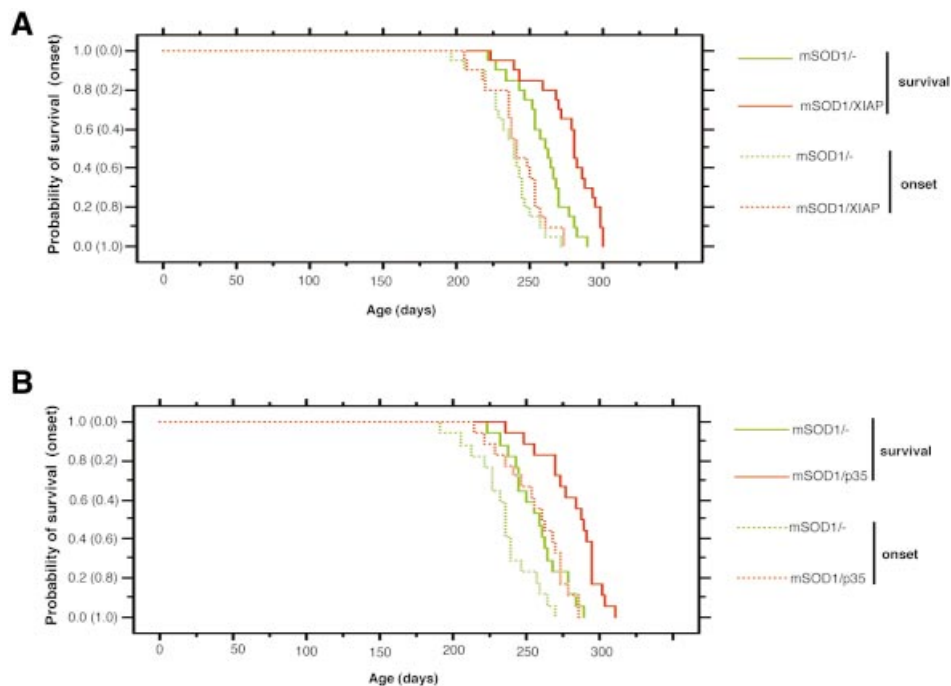


Fig. 2. Age comparison at the end stage of disease (survival) and at the onset of motor deficit scored by rota-rod test (onset) in mSOD1/XIAP-Tg (A) and mSOD1/p35-Tg (B) mice. (A) Probability of survival revealed an extended life span in mSOD1/XIAP-Tg ($n = 20$; red solid line) compared with mSOD1-Tg mice ($n = 20$; green solid line). The cumulative probability of onset of rota-rod deficit was not significantly changed in mSOD1/XIAP-Tg ($n = 20$; red dotted line) compared with mSOD1-Tg mice ($n = 20$; green dotted line). (B) Probability of survival showed an extended life span in mSOD1/p35-Tg ($n = 17$; red solid line) compared with mSOD1-Tg mice ($n = 18$; green solid line). Disease onset, scored by rota-rod test, was delayed in mSOD1/p35-Tg ($n = 17$; red dotted line) compared with mSOD1-Tg mice ($n = 18$; green dotted line). The data were analyzed using the Kaplan–Meier life test and the log-rank test.

and increased gradually right to the end stage (Figure 4A). Caspase-7 activation was detected only after the onset (at 8 months) (Figure 4A).

Next, we examined caspase-9 activation at 6 months in both mSOD1/XIAP-Tg and mSOD1/p35-Tg mice (Figure 4B) because different effects were observed in XIAP and p35 during the clinical course of mSOD1-Tg mice (Figure 2). In mSOD1/p35-Tg mice's spinal cords at 6 months, no caspase-9 activation was observed (Figure 4B); however, caspase-9 activation was observed in the end stage (Figure 4C). These data suggest that p35 delayed caspase-9 activation by inhibiting upstream caspase(s) leading to caspase-9 activation, although the nature of such caspase(s) is unknown. As a sharp drop of procaspase-3 did not occur in mSOD1/p35-Tg mice spinal cords at 6 months, p35 may inhibit an unidentified upstream caspase(s) of caspase-3 other than caspase-9 (Figure 4B). Caspase-9 activation, however, was observed in mSOD1/XIAP-Tg mice at 6 months, although to a lesser extent compared with that in mSOD1-Tg mice (Figure 4B).

A serial examination of caspase-9 activation in mSOD1/XIAP-Tg mice (Figure 4C) was also performed. Weakened activation of caspase-9 in mSOD1/XIAP-Tg was observed when compared with mSOD1-Tg mice. An immunoprecipitation assay using anti-XIAP antibody revealed a binding between the human XIAP and the caspase-9 in the spinal cord lysates of mSOD1/XIAP-Tg mice (Figure 4D). Caspase-9 activation in spinal motor neurons of mSOD1-Tg mice was confirmed by double staining with a neuron-specific antibody (NeuN) and an antibody for activated caspase-9 (Figure 4E). These data

strongly suggest that the inhibition of caspase-9 by XIAP in motor neurons attenuates disease progression.

These results are confirmed by *in vitro* data (Ryan *et al.*, 2002) showing that p35 does not inhibit caspase-9, while XIAP does (Srinivasula *et al.*, 2001). Ac-YVAD-MCA (caspase-1-like), Ac-DEVD-MCA (caspase-3- or -7-like) and Ac-LEHD-MCA (caspase-9-like) cleavage activities, showing the catalytic activity of these caspases, were elevated in the lumbar spinal cords of mSOD1-Tg mice, which was consistent with western blot results (Figure 4F). In mSOD1/XIAP or mSOD1/p35-Tg mice, the presence of XIAP or p35 resulted in a significant reduction of all caspase-like activities tested (Figure 4F). Reduced caspase-1 activity in mSOD1/XIAP-Tg mice as compared with that in mSOD1-Tg mice is probably due to the delay of glial response against neuronal cell death accompanying caspase-1 activation. On the other hand, reduced caspase-9 activity in mSOD1/p35-Tg mice suggests that p35 delays the activation of caspase-9, as shown in Figure 4B. p35-mediated inhibition of caspase-1, caspase-3, or another unidentified caspase(s) upstream of caspase-9 activation may be responsible for this effect.

Caspase-9 is activated in ALS spinal cords

To examine possible caspase-9-activation in human sporadic ALS, we performed immunohistochemistry using anti-active caspase-9 antibody on post mortem human samples. Four of the eight ALS spinal cords showed obvious caspase-9 activation in the motor neurons studied, but this was not seen in any of the controls (Figure 5A); this suggests that caspase-9 may play an

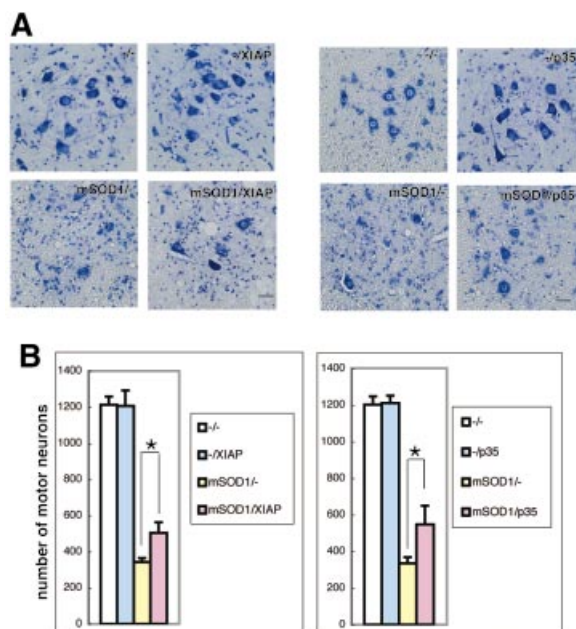


Fig. 3. Protective effects of XIAP or p35 against mutant SOD1 neurotoxicity. (A) Cresyl violet-stained paraffin sections of ventral horn from the lumbar spinal cord revealed a markedly reduced number of motor neurons in mSOD1-Tg mice at end stage, whereas age-matched mSOD1/XIAP-Tg or mSOD1/p35-Tg mice displayed a higher number of motor neurons. Non-Tg, XIAP-Tg and p35-Tg mice showed a similar number of healthy motor neurons. Scale bar = 30 μ m. (B) Quantitative graph showing a significant decrease in the number of large neurons from the anterior horn at the end stage of mSOD1-Tg mice, between levels L3 and L4, compared with age-matched mSOD1/XIAP-Tg or mSOD1/p35-Tg mice ($n = 3-7$ in each group). * $p < 0.05$, according to ANOVA followed by Fisher's test. Error bars represent the SEM.

instrumental role in some forms of human sporadic ALS. To control for the temporal effects of death prior to autopsy, immunohistochemistry was undertaken using anti-procaspase-9 antibody that does not cross-react with the active form of caspase-9. This showed that procaspase-9 is expressed in spinal motor neurons of control patients (data not shown). To determine whether caspase-9 is activated in spinal cords in ALS in a quantitative manner, we performed caspase-9-like activity assay. Caspase-9-like activity in ALS anterior horn was 230.2% of control (Figure 5B).

Discussion

The neurodegenerative process of ALS mouse models is pathologically characterized by chronic activation of caspase-1 and the involvement of mitochondria-dependent cell death pathways (Friedlander, 2003; Guégan and Przedoborski, 2003): Bax translocation from cytosol to the mitochondria, cytochrome *c* release, subsequent caspase-9, and downstream caspase-7 activation in spinal cords (Guégan *et al.*, 2001). However, the significance of caspase activation downstream of cytochrome *c* release from the mitochondria has yet to be clarified.

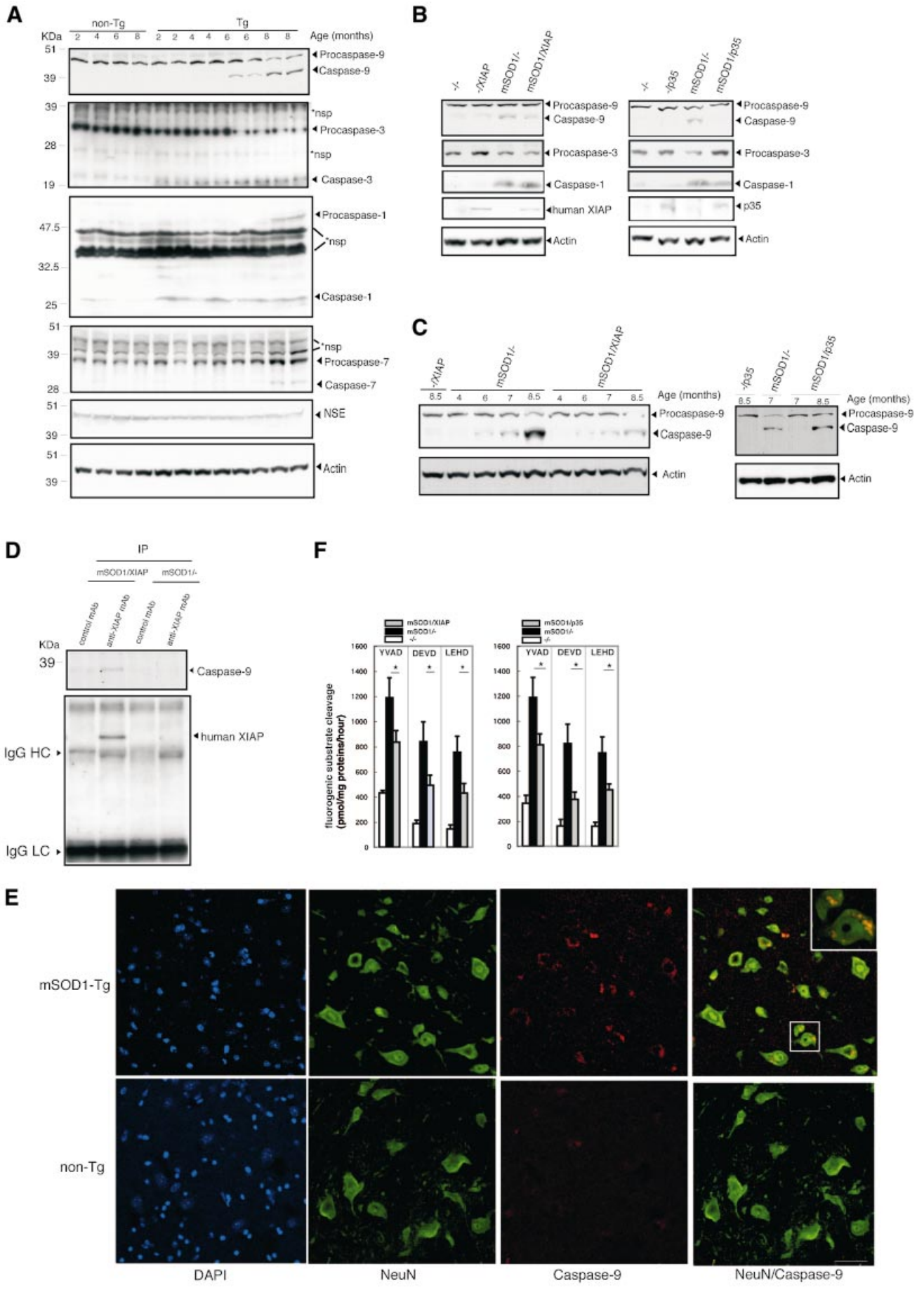
There have been a number of successful therapeutic trials with mutant SOD1 mice. The most dramatic extension of lifespan reported (66.3%) was obtained when mSOD1(G37R)-Tg mice were crossed with neuro-

filament heavy chain-Tg mice (Couillard-Despres *et al.*, 1998). Anti-apoptotic therapies [using the transgene of bcl-2 (Kostic *et al.*, 1997), injection of minocycline (Zhu *et al.*, 2002), intracerebroventricular administration of a synthetic broadcaspase inhibitor zVAD-fmk (Li *et al.*, 2000) or the transgene of dominant-negative caspase-1 (Friedlander *et al.*, 1997)] reportedly show beneficial effects. The extent of prolonged survival achieved with these approaches varied from 8.3% (dominant-negative caspase-1) to 21.6% (zVAD-fmk). Compared with these anti-cell-death therapies, XIAP and p35 transgenes in the present study provided modest benefits (6.8% and 9.5%, respectively). However, the XIAP transgene in this study demonstrated a remarkable effect on disease duration (53.1%).

XIAP expression in motor neurons significantly slows disease progression, whereas p35, a broad caspase inhibitory protein, does not. A previous report showed that zVAD-FMK, another broad caspase inhibitor that inhibits both XIAP- and p35-inhibitable caspases, not only delays onset but also slows disease progression (Li *et al.*, 2000). These findings indicate that different caspases contribute to disease manifestation in preclinical and clinical stages of mouse ALS. Of the XIAP-inhibitable caspases, including caspase-3, -7 and -9, only caspase-9 is not inhibitable by p35 (for a review see Ekert *et al.*, 1999). Moreover, XIAP is physically associated with caspase-9 (for a review see Deveraux and Reed, 1999) (Figure 4D), strongly suggesting that activation of caspase-9 within motor neurons is instrumental in the progression of ALS. Hence, as XIAP levels decrease in spinal motor neurons of mutant SOD1 mice during disease progression (Ishigaki *et al.*, 2002), caspase-9-initiated apoptosis may be promoted.

Caspase-9 is an initiator caspase that primarily processes procaspase-3 into active caspase-3, an effector caspase. Active caspase-3 then activates another set of effector caspases such as caspase-6 and -7, thus bringing about full-blown apoptosis (for a review see Yuan and Yankner, 2000). Based on this scheme, the inhibition of caspase-3 should have the same effect as the inhibition of caspase-9. However, p35, which potently inhibits caspase-3, does not slow disease progression in mouse ALS. There are two explanations for this apparent discrepancy. Since caspase-9 remains active in the presence of p35, procaspase-3 may be continuously processed into active caspase-3, finally overriding inhibition by p35. Alternatively, caspase-9 may utilize a substrate other than caspase-3, leading to caspase-3-independent cell death (Sperandio *et al.*, 2000). Given these possibilities, it is interesting that t-Bid-induced cell death is inhibited by XIAP but not p35 in cultured cells (data not shown), as t-Bid causes the permeability transition of mitochondria and is reportedly seen in motor neurons of mutant SOD1 mice when symptoms start to manifest (Guégan *et al.*, 2002).

Although the level of caspase-9 is higher in 6-month-old mSOD1-Tg mice than in mSOD1/XIAP-Tg mice, the timing of disease onset for both was about the same (Figures 2 and 4B). Caspase-9 activation is mainly triggered by cytochrome *c* release from the mitochondria, which occurs at the asymptomatic stage prior to disease onset (Guégan *et al.*, 2001). Cytochrome *c*, together with ATP/ADP, Apaf-1 and procaspase-9, forms a complex



termed ‘apoptosome’, in which caspase-9 is activated. Caspase-9 then cleaves procaspase-3 to generate active caspase-3. Both caspase-9 and caspase-3 cleave procaspase-9 to form an ‘amplification loop’ of caspase-9 activation (Srinivasula *et al.*, 1998). XIAP does not inhibit ‘apoptosome’ formation and its upstream events, but

suppresses the downstream ‘amplification loop’ by inhibition of caspase-9 and -3. Therefore, the activation of caspase-9 preceded by cytochrome *c* release can occur in the presence of a potent caspase-9 inhibitor XIAP and be considered an indicator of disease onset, regardless of the level of caspase-9.

It should be noted that while XIAP slowed disease progression, it did not completely stop the disease. Although this may stem, in part, from an insufficient amount of XIAP, the caspase-9-activity-independent mitochondrial pathway will be the primary reason for this. Following the permeability transition of mitochondria, both caspase-dependent and -independent cell death signals are generated, and evidence has shown that caspase inhibitors can retard, but not block cell death (for a review see Vila and Przedborski, 2003) following it. Ways of obtaining better treatments, reagents or manipulations that suppress the non-apoptotic process should be identified and used in combination with caspase inhibitors.

Also of note is the fact that XIAP and p35 transgenes were expressed in a neuron-specific manner in this study. An earlier report showed that caspase-1 and -3 are activated not only in motor neurons, but also in glial cells (Li *et al.*, 2000; Pasinelli *et al.*, 2000). Moreover, neuron-specific expression of mutant SOD1 in mice does not lead to the ALS phenotype (Pramatarova *et al.*, 2001; Lino *et al.*, 2002), suggesting that active caspases in non-neuronal cells contribute significantly to disease manifestation. In this regard, caspase inhibition in a broader range of cell types may lead to more marked therapeutic effect in the ALS mouse, as suggested in the study reporting the use of zVAD-FMK (Li *et al.*, 2000). Nevertheless, our data have clearly shown that inhibition of neuronal caspases is sufficient to obtain significant prolongation of survival, implying that caspases are at least partially involved in motor neuronal death through cell-autonomous mechanisms, as suggested in previous reports (Friedlander *et al.*, 1997; Kostic *et al.*, 1997; Raoul *et al.*, 2002).

Taken together, our results indicate that an XIAP-inhibitable caspase, presumably caspase-9, plays an essential role in disease progression in the ALS mouse model. Moreover, we demonstrated that caspase-9 is activated in spinal motor neurons from human ALS patients, suggesting that caspase-9 plays a similar role in the clinical course of human ALS. Since patients with ALS

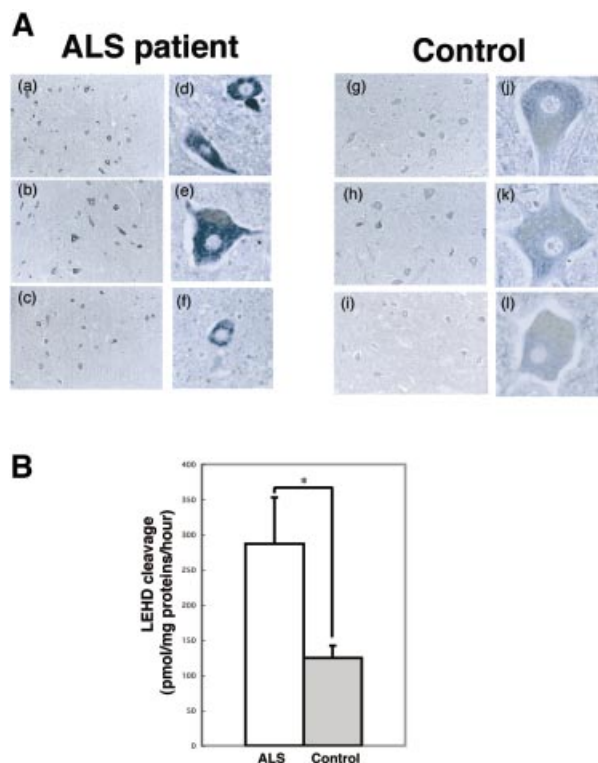


Fig. 5. (A) Immunostaining for the active form of caspase-9 in spinal cord of ALS patients and controls. Immunostaining for the active form of caspase-9 was processed on spinal cord sections obtained from ALS subjects (a–f; $n = 3$) and controls (g–l; $n = 3$). Original magnification $\times 33$ (a–c, g–i) or $\times 100$ (d–f, j–l). In controls, active form caspase-9 displayed faint staining. In ALS cases, some neurons exhibit a normal appearance, whereas most others are much more intensely stained compared with background signal intensity. (B) Activation of caspase-9 in ALS anterior horn. Caspase-9 activity, expressed in pmol of AMC released per milligram of protein per hour, was evaluated using Ac-LEHD-MCA substrate in ALS (white column) and control (gray column) samples. Results are expressed as mean \pm SEM ($n = 5$ per group). $*p < 0.05$ (Student’s *t*-test).

Fig. 4. (A) Caspase-1, -3, -7, -9, neuron-specific enolase (NSE) and actin expression in spinal cords of mSOD1-Tg mice. Western blot of spinal cord lysates from 2-, 4-, 6- and 8-month-old mSOD1-Tg mice. At 2 months, activation of caspase-1 and -3 was detected, but not of caspase-9 and -7. At 6 months, activation of caspase-9 was detected, while at 8 months, activation of caspase-7 was detected. At 8 months, NSE expression was still present. *nsp, non-specific band(s). (B) Representative western blot analysis revealed that the timing of caspase-9 activation in mSOD1/XIAP-Tg mice was not changed. In contrast, activation of caspase-9 was not observed in mSOD1/p35-Tg mice at 6 months. Procaspase-3 decrease is also observed in mSOD1/XIAP-Tg, but not in mSOD1/p35-Tg mice. (C) Attenuation of caspase-9 activation was detected in mSOD1/XIAP-Tg compared with that in mSOD1-Tg mice. Conversely, delayed caspase-9 activation was observed in mSOD1/p35-Tg mice compared with that in mSOD-Tg mice. (D) Interaction between XIAP and caspase-9. Transgene of human XIAP associated with the endogenous active form of caspase-9 is expressed only in diseased mice. IgG HC and IgG LC, bands for heavy chain and light chain immunoglobulin G, respectively. (E) Caspase-9 expression in spinal motor neurons was detected using immunofluorescence staining. Ventral horn sections were stained using an α -NeuN antibody and an antibody to the active form of caspase-9. Merged images show caspase-9 staining mostly in NeuN-positive cells, but also in NeuN-negative cells. Caspase-9 staining was barely detectable in spinal cord sections from non-Tg mice. Staining images are representative of 6-month-old mSOD1-Tg and non-Tg mice. A magnified lesion in the merged image is surrounded by a white square. Scale bar = 40 μ m. (F) Reduction of YVAD-, DEVD- and LEHD-cleaving activities in mSOD1/XIAP-Tg or mSOD1/p35-Tg mice lumbar spinal cords. At 8 months of age, lumbar spinal cord lysates were prepared from XIAP-Tg, p35-Tg, mSOD1-Tg, mSOD1/XIAP-Tg or mSOD1/p35-Tg mice. Caspase-1-, -3-, or -7- and -9-like enzyme activities were measured using fluorogenic substrates Ac-YVAD-MCA (YVAD), Ac-DEVD-MCA (DEVD) and Ac-LEHD-MCA (LEHD), respectively, in the lysates ($n = 6$ –7 mice per group). Data are represented as mean \pm SEM. $*p < 0.05$ indicates a statistically significant difference (ANOVA followed by Fisher’s test). Error bars represent the SEM.

visit clinics after onset of the disease, therapeutic interventions that effectively extend the duration of the disease rather than delaying onset, would appear to offer greater practical benefit. In this regard, caspase-9 represents an excellent target for the treatment of human ALS patients.

Materials and methods

Mice breeding

ChAT-XIAP (or ChAT-Cre) cassettes were microinjected into C57BL/6 pronuclei. The background of loxP-p35 mice was C57BL/6. Transgenic mice (mSOD1-Tg mice) with the G93A human SOD1 mutation (GIL/+) were obtained from Jackson Laboratories (Bar Harbor, ME). The mSOD1-Tg mice were backcrossed to C57BL/6 mice 4 generations. To examine onset and survival, female XIAP (or p35)-Tg mice were crossed with a male mSOD1-Tg mouse. Consequently, we examined data from the fifth backcrossed mice. Moreover, to circumvent potential difficulties caused by genetic backgrounds of mice, transgenic littermates were utilized in the present study. Same-sex members of each litter were housed in the same cage. Food and water were placed at the bottom of the cage allowing *ad libitum* access. All mice were maintained at the animal facilities of RIKEN-BSI according to the guidelines of the institution.

Genotyping of mice

Genotypes were determined using Southern blot analysis and/or PCR. PCR primer sets for mSOD1-Tg mice (S1, S2), XIAP-Tg mice (X1, X2), ChAT-Cre mice (C1, C2) and loxP-p35 mice (P1) were, respectively: S1 forward: 5'-GCAACAGACAGACCTTTGTGTGAC-3', S1 reverse: 5'-GACAGTGTATCACAAAGCCTTCC-3'; S2 forward: 5'-CAT-CAGCCCTAATCCATCTGA-3', S2 reverse: 5'-CG GACTAACAAT-CAAAGTGA-3'; X1 forward: 5'-ACTGTGGCAGGAACACAG-3', X1 reverse: 5'-CAGTGTGATGCTGAAACAGG-3'; X2 forward: 5'-GTACTGAAGAGCAGCTAAGG-3', X2 reverse: 5'-CAGACCTTG-CATTCCTTTGG-3'; C1 forward: 5'-GCAGTTCATGGAAGCAGG-3', C1 reverse: 5'-ACCGCAACCGGACAGAAAG-3'; C2 forward: 5'-CTGGAGTTTCAATACCGGAG-3', C2 reverse: 5'-CAGACCTTG-CATTCCTTTGG-3'; P1 forward: 5'-TGGATGGATTCCACGATAGC-3', P1 reverse: 5'-TGCACACTCTCCACGTAAGC-3'.

Determination of disease onset and progression

Onset was determined as the age at which motor deficits were manifested as an inability to remain on rota-rod treadmills (Accelerating Model; Ugo Basile Biological Research Apparatus, Varese, Italy). Performance was determined at 1-week intervals throughout disease progression. Each trial lasted a maximum of 10 min, during which time the rota-rod underwent linear acceleration from 16 to 32 r.p.m. over the first 5 min of the trial, remaining at maximum speed for the remaining 5 min. Animals were scored for fall latency in each trial. Mortality was scored as date of death or inability of the mouse to right itself within 30 s. Scorers were unaware of the genotypes of the mice or their birth dates.

Histochemistry

For immunohistochemistry, mice were perfused with cold phosphate-buffered saline (PBS) followed by 4% paraformaldehyde in PBS. The spinal cord was removed, embedded in paraffin, sectioned (4 μ m), deparaffinized using standard protocols and stained with specific antibodies such as anti-p35 polyclonal antibody (pAb) (1:500) (Tomioka *et al.*, 2002), anti-human-specific XIAP pAb (1:50; see below), anti-active form of caspase-9 pAb (1:50; Cell Signaling) and anti-NeuN monoclonal antibody (mAb) (1:1000; Chemicon, Temecula, CA). The anti-human-specific XIAP pAb was used to detect not murine, but human XIAP expression. Briefly, the antibody was produced in rabbits by immunization with a peptide, VENYLGSRDHFAL, corresponding to residues in a human-specific region of XIAP. The primary antisera were affinity purified with recombinant protein of human XIAP coding the first baculovirus IAP repeat domain. The specificity of the antibody was tested by western blotting using extract of human or murine XIAP-overexpressing 293T cells (data not shown). Immunoreactivity was visualized using diaminobenzidine after signal amplification using Vectastain ABC Elite (Vector Laboratories, Burlingame, CA) or TSA-indirect reagent (NEL Life Science Products, MA). Double staining for caspase-9 and NeuN was performed as described previously (Li *et al.*, 2000; Guegan *et al.*, 2001). Number of motor neurons was counted as described previously (Oppenheim *et al.*, 2001), with some modification.

Spinal cords were embedded in paraffin and serially sectioned (14 μ m) from L3 to L4 (Sidman *et al.*, 1971). Motor neurons were counted in every fifth section through each population examined, and totals were multiplied by five to give an estimate of total cell numbers.

Hypoglossal nerve axotomy

Female mice (3-months-old) were anesthetized using pentobarbital sodium, then operated on under sterile conditions. The right hypoglossal nerve was transected under the digastric muscle. As positive control, a $3 \times 3 \times 2$ mm³ piece of spongel (Yamanouchi Pharmaceutical, Tokyo, Japan) soaked in 2.8 mg/ml of BDNF (Sumitomo Pharmaceutical, Osaka, Japan) in PBS, or PBS alone, was implanted into the nerve stump for local administration at the time of surgery, as described previously (Yan *et al.*, 1994). After 6 weeks, mice were deeply anesthetized with chloral hydrate and perfused with cold PBS, pH 7.4, followed by 4% paraformaldehyde in PBS. Brains were removed, post-fixed for 2–3 days and cryoprotected. Forty-micrometer thick serial sections were cut on a cryotome and stained using cresyl violet. Total number of motor neurons in the hypoglossal nerve nuclei was counted using unbiased stereological methods.

Northern blot analysis

To confirm XIAP mRNA expression, northern blot analysis was performed as follows: 20 μ g of total RNA was separated on a 1.5% agarose gel containing 0.66 M formaldehyde, then transferred to a Duraron-UV membrane (Stratagene, La Jolla, CA) according to the manufacturer's instructions. Filters were baked at 80°C for 2 h. PCR was used to amplify cDNAs of ~300 bp, which were then labeled with [³²P]dCTP. Membrane filters were hybridized with labeled probes (1 \times 10⁶ c.p.m./ml) in buffer (40% deionized formamide, 4 \times SSC, 10% dextran sulfate, 1 \times Denhardt's solution, 40 μ g/ml sonicated and denatured salmon sperm DNA, 0.1% SDS, 20 mM Tris pH 7.5) at 42°C for 16 h. Filters were washed twice for 15 min at room temperature and once for 30 min at 56°C with 2 \times SSC containing 0.1% SDS, then exposed.

Western blot analysis

Spinal cord lysates were prepared in RIPA buffer (150 mM NaCl, 1% NP-40, 0.5% deoxycholate, 0.1% SDS, 50 mM Tris, pH 8.0). Protein concentration was determined using BCA protein assay (Pierce, Rockford, IL). Protein from tissue lysates were separated on a polyacrylamide gel, blotted on a PVDF filter, stained with anti-XIAP pAb (1:100; R&D Systems, Minneapolis, MN) which recognizes both human and murine XIAP, anti-human-specific XIAP pAb which is also used in histochemistry, anti-caspase-1 pAb (1:100; Santa Cruz Biotechnology, Santa Cruz, CA), anti-caspase-3 pAb (1:100; see below), anti-caspase-7 pAb (1:100; R&D Systems), anti-caspase-9 pAb (1:1000; StressGen Biotechnologies, Victoria, Canada), anti-neuron-specific enolase (NSE) mAb (1:1000; DakoCytomation, Kyoto, Japan) and anti-actin mAb (1:5000; Santa Cruz Biotechnology), and autoradiographed using enhanced chemiluminescence (Amersham Pharmacia Biotech, Piscataway, NJ). The anti-caspase-3 pAb was generated according to a previous report (Kourouk *et al.*, 1998).

RT-PCR

To confirm p35 mRNA expression under Cre-recombinase-expressing conditions, RT-PCR was performed. Total RNAs were prepared from 2-month-old mice spinal cords using ISOGEN (Nippon Gene, Tokyo, Japan). RNAs were reverse-transcribed using SuperScript II reverse transcriptase (Gibco-BRL, Rockville, MD) according to the manufacturer's instructions. Following heat inactivation of reverse transcriptase, the cDNA was amplified using ExTaq DNA polymerase (TaKaRa, Tokyo, Japan). Primers used for amplification were: forward, 5'-TCTGACT-GACCGCTTACTCC-3' (neo2); reverse 5'-TGCACACTCTCCACG-TAAGC-3' (p35-4).

Caspase activity assay

Caspase activities were assayed as described previously (Kanuka *et al.*, 1999; Suzuki *et al.*, 2001) with some modification. Freshly isolated spinal cords were pulverized in a liquid-nitrogen-chilled mortar. Frozen spinal cords were homogenized in 50 mM Tris pH 7.5, 1 mM EDTA, 10 mM EGTA and 10 μ M digitonin. Homogenates were incubated at 37°C for 10 min, and clarified by centrifugation at 15 000 g for 10 min. The cleared lysates containing 50 μ g protein were mixed with assay buffer {20 mM Pipes, 100 mM NaCl, 1 mM EDTA, 0.1% 3-[(3-cholamidopropyl)dimethylammonio]-1-propanesulfonate, 10% sucrose, 10 mM DTT, pH 7.2} and preincubated at 37°C for 15 min (1.0 mg/ml final protein concentration). Assay buffer (50 μ l) containing 200 μ M enzyme substrate

Ac-YVAD-MCA, Ac-DEVD-MCA or Ac-LEHD-MCA (Peptide Institute, Osaka, Japan) was added to the lysate. Activity was measured continuously over the time indicated by the release of 7-amino-4-methylcoumarin (AMC) from each substrate as emission at 460 nm and excitation at 355 nm using a fluorometer, Fluoroskan Ascent FL (Labsystems, Chicago, IL) in the kinetic mode. Activity was expressed as pmol of AMC generated per hour per milligram of the total protein extract at 37°C.

Immunoprecipitation

Whole spinal cord lysates from 8-month-old mSOD1/XIAP-Tg mice ($n = 3$) and mSOD1-Tg mice ($n = 3$) (1 mg protein) were incubated with 1 µg of control mAb or anti-XIAP mAb (Transduction Laboratories, KY) conjugated with 10 µl of protein G-Sepharose at 4°C for 3 h. Immunoprecipitates were separated on a polyacrylamide gel, transferred to PVDF membrane, and analyzed by immunoblotting using anti-human-specific XIAP pAb (1:50) or anti-caspase-9 pAb (1:1000; StressGen Biotechnologies).

Human samples

Patients were diagnosed as having ALS by clinical and/or neuropathological criteria (Kuncl *et al.*, 1992). None of the ALS patients had a family history of the illness. At autopsy, spinal cords were removed and blocks of each level of spinal cord were immediately placed in 10%-buffered formalin, embedded in paraffin, and subjected to neuropathological examination, or immediately frozen, and subjected to biochemical examination.

For immunohistochemistry, the tissues used originated from eight spinal cord samples from patients with ALS and three from neurological patients with no spinal cord pathology. Causes of death were respiratory arrest ($n = 8$) in the ALS group and cerebrovascular disease ($n = 3$) in the control group. The mean differences between the time from death to autopsy for ALS and control groups were 9.1 ± 6.4 and 6.3 ± 4.9 h, respectively (mean \pm SD). The mean ages for ALS and control groups were 70.8 ± 3.3 and 73.7 ± 4.5 years, respectively. The clinical diagnosis of ALS was confirmed pathologically in all eight ALS patients. In these spinal cord specimens, severe neuronal loss was recorded in the anterior horn with mild to moderate gliosis, whereas no remarkable pathological changes were noted in spinal cords from controls.

For caspase-9-like activity assay, the tissues used originated from five spinal cord samples from patients with ALS and five from age-matched control individuals. Causes of death were respiratory arrest ($n = 4$) and pneumonia ($n = 1$) in the ALS group, and pneumonia ($n = 2$), lung carcinoma ($n = 1$), lung abscess ($n = 1$) and heart failure ($n = 1$) in the control group. Samples of spinal cord included only the anterior horn gray matter (mostly the group IX column) of lumbar levels as described previously (Martin, 1999). Frozen tissue samples from ALS ($n = 5$) and control ($n = 5$) cases were homogenized and LEHD cleavage (caspase-9-like) activity was assayed as described above. The post mortem delays for the ALS and control groups were 4.8 ± 1.6 and 6.6 ± 4.0 h, respectively. The mean ages for ALS and control groups were 66.0 ± 13.5 and 70.0 ± 6.7 years, respectively.

Acknowledgements

The authors wish to thank: J.Miyazaki for CAG-CAT-Z mice; Y.Nagaoka for mouse embryo manipulation; M.Katayama for histology; T.Usami, T.Yoda and M.Shichita for technical support; M.Urushitani, C.Nakayama and K.Shirota for advice on experiments; H.Kanuka for the anti-caspase antibody; H.Hayashi and T.Mizutani for human samples; J.Matsuura for instruction in axotomy; and B.L.La Madeleine for editing the manuscript. This work was supported by research grants from RIKEN BSI, a Grant-in-Aid for Scientific Research on Priority Areas (Advanced Brain Science Project) from the Ministry of Education, Culture, Sports, Science and Technology, Japan, a Grant-in-Aid for Encouragement of Young Scientists, a Grant-in-Aid for Encouragement of Young Scientists, and a Grant-in-Aid from the Nakabayashi Trust For ALS Research.

References

Brown,R.H.,Jr and Robberecht,W. (2001) Amyotrophic lateral sclerosis: pathogenesis. *Semin. Neurol.*, **21**, 131–139.
 Cleveland,D.W. and Rothstein,J.D. (2001) From Charcot to Lou Gehrig: deciphering selective motor neuron death in ALS. *Nat. Rev. Neurosci.*, **2**, 806–819.

Couillard-Despres,S., Zhu,Q., Wong,P.C., Price,D.L., Cleveland,D.W. and Julien,J-P. (1998) Protective effect of neurofilament heavy gene overexpression in motor neuron disease induced by mutant superoxide dismutase. *Proc. Natl Acad. Sci. USA*, **95**, 9626–9630.
 Crocker,S.J. *et al.* (2003) Attenuation of MPTP-induced neurotoxicity and behavioural impairment in NSE-XIAP transgenic mice. *Neurobiol. Dis.*, **12**, 150–161.
 Deveraux,Q.L. and Reed,J.C. (1999) IAP family proteins-suppressors of apoptosis. *Genes Dev.*, **13**, 239–252.
 Deveraux,Q.L., Leo,E., Stennicke,H.R., Welsh,K., Salvesen,G.S. and Reed,J.C. (1999) Cleavage of human inhibitor of apoptosis protein XIAP results in fragments with distinct specificities for caspases. *EMBO J.*, **18**, 5242–5251.
 Ekert,P.G., Silke,J. and Vaux,D.L. (1999) Caspase inhibitors. *Cell Death Differ.*, **6**, 1081–1086.
 Friedlander,R.M. (2003) Apoptosis and caspases in neurodegenerative diseases. *N. Engl. J. Med.*, **348**, 1365–1375.
 Friedlander,R.M., Brown,R.H.,Jr, Gagliardini,V., Wang,J. and Yuan,J. (1997) Inhibition of ICE slows ALS in mice. *Nature*, **388**, 31.
 Guégan,C. and Przedborski,S. (2003) Programmed cell death in amyotrophic lateral sclerosis. *J. Clin. Invest.*, **111**, 153–161.
 Guégan,C., Vila,M., Rosoklija,G., Hays,A.P. and Przedborski,S. (2001) Recruitment of the mitochondrial-dependent apoptotic pathway in amyotrophic lateral sclerosis. *J. Neurosci.*, **21**, 7569–7576.
 Guégan,C., Vila,M., Teissman,P., Chen,C., Onteniente,B., Li,M., Friedlander,R.M. and Przedborski,S. (2002) Instrumental activation of Bid by caspase-1 in a transgenic mouse model of ALS. *Mol. Cell. Neurosci.*, **20**, 553–562.
 Gurney,M.E. *et al.* (1994) Motor neuron degeneration in mice that express a human Cu, Zn superoxide dismutase mutation. *Science*, **264**, 1772–1775.
 Gurney,M.E., Tomasselli,A.G. and Heinrikson,R.L. (2000) Stay the executioner's hand. *Science*, **288**, 283–284.
 Hayward,L.J., Rodriguez,J.A., Kim,J.W., Tiwari,A., Goto,J.J., Cabelli,D.E., Valentine,J.S. and Brown,R.H.,Jr (2002) Decreased metallation and activity in subsets of mutant superoxide dismutases associated with familial amyotrophic lateral sclerosis. *J. Biol. Chem.*, **277**, 15923–15931.
 Hisahara,S. *et al.* (2000) Targeted expression of baculovirus p35 caspase inhibitor in oligodendrocytes protects mice against autoimmune-mediated demyelination. *EMBO J.*, **19**, 341–348.
 Howland,D.S. *et al.* (2002) Focal loss of the glutamate transporter EAAT2 in a transgenic rat model of SOD1 mutant-mediated amyotrophic lateral sclerosis (ALS). *Proc. Natl Acad. Sci. USA*, **99**, 1604–1609.
 Ishigaki,S., Liang,Y., Yamamoto,M., Niwa,J., Ando,Y., Yoshihara,T., Takeuchi,H., Doyu,M. and Sobue,G. (2002) X-linked inhibitor of apoptosis protein is involved in mutant SOD1-mediated neuronal degeneration. *J. Neurochem.*, **82**, 576–584.
 Julien,J-P. (2001) Amyotrophic lateral sclerosis: unfolding the toxicity of the misfolded. *Cell*, **104**, 581–591.
 Kanuka,H., Hisahara,S., Sawamoto,K., Shoji,S., Okano,H. and Miura,M. (1999) Proapoptotic activity of *Caenorhabditis elegans* CED-4 protein in *Drosophila*: Implicated mechanisms for caspase activation. *Proc. Natl Acad. Sci. USA*, **96**, 145–150.
 Kostic,V., Jackson-Lewis,V., Bilbao,F., Dubois-Dauphin,M. and Przedborski,S. (1997) Bcl-2: Prolonged life in a transgenic mouse model of familial amyotrophic lateral sclerosis. *Science*, **277**, 559–562.
 Kouroku,Y., Urase,K., Fujita,E., Isahara,K., Ohsawa,Y., Uchiyama,Y., Momoi,M.Y. and Momoi,T. (1998) Detection of activated Caspase-3 by a cleavage site-directed antiserum during naturally occurring DRG neurons apoptosis. *Biochem. Biophys. Res. Commun.*, **247**, 780–784.
 Kügler,S., Straten,G., Kreppel,F., Isenmann,S., Liston,P. and Bahr,M. (2000) The X-linked inhibitor of apoptosis (XIAP) prevents cell death in axotomized CNS neurons *in vivo*. *Cell Death Differ.*, **7**, 815–824.
 Kuncl,R.W., Crawford,T.O., Rothstein,J.D. and Drachman,D.B. (1992) Motor neuron diseases. In Asbury,A.K., McKhann,G.M. and McDonald,W.I. (eds), *Diseases of the Nervous System. Clinical Neurobiology*. WB Saunders, Philadelphia, PA, pp. 1179–1208.
 Li,M. *et al.* (2000) Functional role of caspase-1 and caspase-3 in an ALS transgenic mouse model. *Science*, **288**, 335–339.
 Lino,M.M., Schneider,C. and Caroni,P. (2002) Accumulation of SOD1 mutants in postnatal motoneurons does not cause motoneuron pathology or motor neuron disease. *J. Neurosci.*, **22**, 4825–4832.
 Martin,L.J. (1999) Neuronal death in amyotrophic lateral sclerosis is apoptosis: possible contribution of a programmed cell death mechanism. *J. Neuropathol. Exp. Neurol.*, **58**, 459–471.

- Naciff, J.M., Behbehani, M.M., Misawa, H. and Dedman, J.R. (1999) Identification and transgenic analysis of a murine promoter that targets cholinergic neuron expression. *J. Neurochem.*, **72**, 17–28.
- Oppenheim, R.W. *et al.* (2001) Cardiotrophin-1, a muscle-derived cytokine, is required for the survival of subpopulations of developing motoneurons. *J. Neurosci.*, **21**, 1283–1291.
- Pasinelli, P., Houseweart, M.K., Brown, R.H., Jr and Cleveland, D.W. (2000) Caspase-1 and caspase-3 are sequentially activated in motor neuron death in Cu, Zn superoxide dismutase-mediated familial amyotrophic lateral sclerosis. *Proc. Natl Acad. Sci. USA*, **97**, 13901–13906.
- Perrelet, D. *et al.* (2000) IAP family proteins delay motoneuron cell death *in vivo*. *Eur. J. Neurosci.*, **12**, 2059–2067.
- Pramatarova, A., Laganier, J., Roussel, J., Brisebois, K. and Rouleau, G.A. (2001) Neuron-specific expression of mutant superoxide dismutase 1 in transgenic mice does not lead to motor impairment. *J. Neurosci.*, **21**, 3369–3374.
- Raoul, C., Estevez, A.G., Nishimune, H., Cleveland, D.W., deLapeyriere, O., Henderson, C.E., Haase, G. and Pettmann, B. (2002) Motoneuron death triggered by specific pathway downstream of Fas: potentiation by ALS-linked SOD1 mutations. *Neuron*, **35**, 1067–1083.
- Rosen, D.R. *et al.* (1993) Mutations in Cu/Zn superoxide dismutase gene are associated with familial amyotrophic lateral sclerosis. *Nature*, **362**, 59–62.
- Rowland, L.P. and Shneider, N.A. (2001) Amyotrophic lateral sclerosis. *N. Engl. J. Med.*, **344**, 1688–1700.
- Ryan, C.A., Stennicke, H.R., Nava, V.E., Burch, J.B., Hardwick, J.M. and Salvesen, G.S. (2002) Inhibitor specificity of recombinant and endogenous caspase-9. *Biochem. J.*, **366**, 595–601.
- Sakai, K. and Miyazaki, J. (1997) A transgenic mouse line that retains Cre recombinase activity in mature oocytes irrespective of the cre transgene transmission. *Biochem. Biophys. Res. Commun.*, **237**, 318–324.
- Sidman, R.L., Angevine, J.B., Jr and Pierce, E.T. (1971) *Atlas of the Mouse Brain and Spinal Cord*. Harvard University Press, Cambridge, MA, pp. 249–261.
- Sperandio, S., Belle, I. and Bredesen, D.E. (2000) An alternative, nonapoptotic form of programmed cell death. *Proc. Natl Acad. Sci. USA*, **97**, 14376–14381.
- Srinivasula, S.M., Ahmad, M., Fernandes-Alnemri, T. and Alnemri, E.S. (1998) Autoactivation of procaspase-9 by Apaf-1-mediated oligomerization. *Mol. Cell*, **7**, 949–957.
- Srinivasula, S.M. *et al.* (2001) A conserved XIAP-interaction motif in caspase-9 and Smac/DIABLO regulates caspase activity and apoptosis. *Nature*, **410**, 112–116.
- Subramaniam, J.R., Lyons, W.E., Liu, J., Bartnikas, T.B., Rothstein, J.D., Price, D.L., Cleveland, D.W., Gitlin, J.D. and Wong, P.C. (2002) Mutant SOD1 causes motor neuron disease independent of copper chaperone-mediated copper loading. *Nat. Neurosci.*, **5**, 301–307.
- Suzuki, Y., Nakabayashi, Y. and Takahashi, R. (2001) Ubiquitin-protein ligase activity of X-linked inhibitor of apoptosis protein promotes proteasomal degradation of caspase-3 and enhances its anti-apoptotic effect in Fas-induced cell death. *Proc. Natl Acad. Sci. USA*, **98**, 8662–8667.
- Tiwari, A. and Hayward, L.J. (2003) Familial amyotrophic lateral sclerosis mutants of copper/zinc superoxide dismutase are susceptible to disulfide reduction. *J. Biol. Chem.*, **278**, 5984–5992.
- Tomioka, M., Shirogami, K., Iwata, N., Lee, H.J., Yang, F., Cole, G.M., Seyama, Y. and Saido, T.C. (2002) *In vivo* role of caspases in excitotoxic neuronal death: generation and analysis of transgenic mice expressing baculoviral caspase inhibitor, p35, in postnatal neurons. *Mol. Brain Res.*, **108**, 18–32.
- Vila, M. and Przedborski, S. (2003) Targeting programmed cell death in neurodegenerative diseases. *Nat. Rev. Neurosci.*, **4**, 1–11.
- Viswanath, V., Wu, Z., Fonck, C., Wei, Q., Boonplueang, R. and Andersen, J.K. (2002) Transgenic mice neurally expressing baculoviral p35 are resistant to diverse types of induced apoptosis, including seizure-associated neurodegeneration. *Proc. Natl Acad. Sci. USA*, **97**, 2270–2275.
- Yan, Q., Matheson, C., Lopez, O.T. and Miller, J.A. (1994) The biological responses of axotomized adult motoneurons to brain-derived neurotrophic factor. *J. Neurosci.*, **14**, 5281–5291.
- Yuan, J. and Yankner, B.A. (2000) Apoptosis in the nervous system. *Nature*, **407**, 802–809.
- Zhu, S. *et al.* (2002) Minocycline inhibits cytochrome *c* release and delays progression of amyotrophic lateral sclerosis. *Nature*, **417**, 74–78.

Received June 24, 2003; revised October 27, 2003;
accepted October 30, 2003